35th Annual International Conference of the IEEE EMBS
Osaka, Japan, 3 - 7 July, 2013

Dynamic Modeling of Respiratory Sinus Arrhythmia Component from HRV with Multivariate Kalman Smoother

P. Kuoppa*[1], J.A. Lipponen[1] and M.P. Tarvainen[1,2]

[1] University of Eastern Finland, Department of Applied Physics, Kuopio, Finland
[2] Kuopio University Hospital, Department of Clinical Physiology and Nuclear Medicine, Kuopio, Finland

Abstract— **The estimates of heart rate variability (HRV) low frequency (LF) and high frequency (HF) components with constant frequency bands may distort when the frequency of respiratory sinus arrhythmia induced HF component approaches the LF-HF frequency limit. In this study we present a method for dynamically estimating the LF-HF limit and dividing the spectrum to LF and HF components that can overlap. The method is based on multivariate autoregressive model which is solved dynamically with Kalman smoother algorithm. The spectra of each individual pole with all the zeros are calculated and then multiplied with a Hanning window on the pole frequency. These spectra are summed to LF or HF components. The method was applied to three subjects whose electrocardiogram and respiration was recorded during a controlled breathing protocol. The results show that the HF component power increases when breathing frequency decreases. Also the component powers obtained with the presented method are reliable even when LF and HF frequencies are close to each other.**

I. INTRODUCTION

Heart rate variability (HRV) analysis is a commonly used tool for assessing the functioning of the autonomic nervous system (ANS). HRV is usually analyzed in frequency domain by dividing the power spectrum of R-to-R peak interval (RR) time series into low frequency (LF, 0.04-0.15 Hz) and high frequency (HF, 0.15-0.40 Hz) bands [1], [2]. The LF component of HRV is thought to originate from both sympathetic and parasympathetic activities. The HF component of HRV originates from parasympathetic regulation of heart rate. The HF component peaks at respiratory frequency because of respiratory sinus arrhythmia (RSA). Therefore, the estimates with constant bands will distort when the frequency of breathing induced HF component approaches the LF-HF frequency limit and leaks to the LF band. Hence the respiratory frequency should always be taken into account in HRV analysis, at least to ensure that the RSA component is within the defined HF band.

In this paper, we introduce a method for dynamical estimation of the LF and HF components of HRV taking into account the instantaneous respiratory frequency. In the proposed method, RR time series and respiration (RSP) signal are modelled using a multivariate autoregressive (MAR) model. This kind of model (or autoregressive moving-average, ARMA) has been previously used to study HRV with mainly blood pressure signal [3], [4], [5], [6], [7], [8].

The model coefficients are estimated for every time step using a Kalman smoother algorithm. From the estimated model coefficients, instantaneous power spectra for HRV and respiration are obtained. Furthermore, the HRV spectrum is divided into LF and HF components at every time step by defining a physiologically meaningful limit for separating the LF and HF components based on the instantaneous respiratory frequency.

Similar decomposition has been done previously with univariate AR model in [9], but the benefits of the MAR modeling are that the dependencies between the two signals can be more precisely evaluated and the HRV spectrum can be estimated more accurately.

II. MATERIALS & METHODS

A. Subjects and measurements

Three young adult males participated in this study. The measurement protocol included the subject sitting in an armchair and breathing in a controlled rate while electrocardiogram (ECG) and RSP signals were recorded from the subject. ECG channel V5 and RSP were measured with ECG100C and RSP100C modules of BIOPAC MP150 data acquisition system (BIOPAC Systems, Inc., Goleta, USA) with sampling rate of 500 Hz.

The breathing protocol consisted of segments of controlled breathing in descending frequencies 0.20, 0.17, 0.13 and 0.10 Hz. Each segment lasted three minutes. Visual and audio indicators of the current frequency was shown to the subject and he was instructed to breath at the same frequency.

B. Pre-processing of the signals

The QRS detection for the ECG was done with Kubios HRV analyzing software [10]. The obtained RR interval time series was interpolated to 4 Hz and the very low frequency (VLF, 0-0.04 Hz) trend components were removed using a smoothness priors detrending method [11]. The RSP signal was down sampled to 4 Hz and the trend was also removed with smoothness priors.

C. Multivariate Kalman smoother

We used multivariate Kalman smoother to analyze the signals spectra dynamically. It consists of filter and smoother algorithms. The filter part is first run forward in time and

*Corresponding author: P. Kuoppa, Department of Applied Physics, University of Eastern Finland, P.O.Box 1627, FI-70211 Kuopio, Finland (pekka.kuoppa@uef.fi).

978-1-4577-0216-7/13/$26.00 ©2013 IEEE

the obtained estimates are used then to run the smoother backwards in time to get the smoothed estimates.

A time-varying multivariate autoregressive model (MAR) of order p can be expressed as

$$x_t = -\sum_{j=1}^{p} A_t^{(j)} x_{t-j} + e_t \tag{1}$$

where x_t is the signal value at time t, $A_t^{(j)}$ is the j'th autoregressive parameter and e_t is the observation error. In a two signal case (RR and RSP) x_t and e_t are vectors

$$x_t = (x_t^1 \; x_t^2)^T \tag{2}$$

$$e_t = (e_t^1 \; e_t^2)^T \tag{3}$$

where x_t^1 and x_t^2 are the signal values at time t for RR and RSP, respectively, and likewise for e_t^1 and e_t^2. The parameter $A_t^{(j)}$ is now a 2×2 matrix

$$A_t^{(j)} = \begin{bmatrix} a_t^{(1,1)} & a_t^{(1,2)} \\ a_t^{(2,1)} & a_t^{(2,2)} \end{bmatrix}^{(j)} \tag{4}$$

where the diagonal values are MAR models auto-coefficients and the off-diagonal ones are cross-coefficients. By denoting

$$H_t = (x_{t-1}, \ldots, x_{t-p}) \tag{5}$$

$$\theta_t = (-A_t^{(1)}, \ldots, -A_t^{(p)})^T \tag{6}$$

we can present equation (1) as a matrix multiplication

$$x_t = H_t \theta_t + e_t \tag{7}$$

which is the linear observation model for the Kalman smoother algorithm. The state model for Kalman smoother is the estimation of MAR parameters with random walk model

$$\theta_{t+1} = \theta_t + w_t \tag{8}$$

where w_t is the state noise.

Using equations (7) and (8) the MAR parameters can be estimated with Kalman filter functions

$$C_{\tilde{\theta}_{t|t-1}} = C_{\tilde{\theta}_{t-1}} + C_{w_{t-1}} \tag{9}$$

$$K_t = C_{\tilde{\theta}_{t|t-1}} H_t^T (H_t C_{\tilde{\theta}_{t|t-1}} H_t^T + C_{e_t})^{-1} \tag{10}$$

$$\hat{\theta}_t = \hat{\theta}_{t-1} + K_t (x_t - H_t \hat{\theta}_{t-1}) \tag{11}$$

$$C_{\tilde{\theta}_t} = (I - K_t H_t) C_{\tilde{\theta}_{t|t-1}} \tag{12}$$

where $\tilde{\theta}_t$ is the state estimation error, $\tilde{\theta}_{t|t-1}$ is the state prediction error, K_t is the Kalman gain vector, and C_{e_t} and C_{w_t} are the observation and state noise covariances, respectively.

The observation noise covariance matrix C_{e_t} is estimated adaptively with function

$$C_{e_t} = 0.95\, C_{e_{t-1}} + 0.05\, \epsilon_t^2 \tag{13}$$

where $\epsilon_t = x_t - H_t \hat{\theta}_{t-1}$ is current prediction error vector, which is used as an estimate of the unknown observation error e_t. The observation noise covariance is also used to calculate the state noise covariance matrix

$$C_{w_t} = \lambda\, C_{e_t} / C_{x_t} \tag{14}$$

where C_{x_t} is the covariance matrix of signals x_t calculated from 100 previous timesteps and λ is a set coefficient to scale the ratio. This way the adaptation speed of the algorithm can be controlled with single variable λ.

The Kalman smoother part is run backwards in time after the filter algorithm has been ran forward in time. The equations for the smoother algorithm are

$$\hat{\theta}_t^{\mathrm{S}} = \hat{\theta}_t + B_t (\hat{\theta}_{t+1}^{\mathrm{S}} - \hat{\theta}_t) \tag{15}$$

$$C_{\tilde{\theta}_t^{\mathrm{S}}} = C_{\tilde{\theta}_t} + B_t (C_{\tilde{\theta}_{t+1}^{\mathrm{S}}} - C_{\tilde{\theta}_{t+1|t}}) B_t^T \tag{16}$$

where $B_t = C_{\tilde{\theta}_t} C_{\tilde{\theta}_{t+1|t}}^{-1}$ and $\hat{\theta}_t^{\mathrm{S}}$ denotes the smoothed parameter estimate for time t. For a closer look at Kalman smoother equations see for example [12].

The initial values for the filter part were obtained by estimating the MAR parameters using the first 40 s to solve equation (1) with least square method for the first time step. Model order $p = 20$ was used for both the initialization and the actual Kalman algorithm. The model order was chosen by visual inspection to produce high enough frequency resolution for the cases when RSP frequency was 0.1 Hz. From the initialization we got $\hat{\theta}_1$, C_{e_1} and C_{x_t}. Adaptation coefficient was set to $\lambda = 10^{-4}$ and $C_{\tilde{\theta}_1} = 0.1I$.

D. MAR spectral estimate

The estimated MAR parameters and observation noise covariance matrix can be used to calculate spectral estimates of the signals for each time step (see for example [13] for more detailed explanation). This can be done by first forming the z-transform of MAR model (1)

$$\mathbf{P}_t(z) = \mathbf{A}_t^{-1}(z) C_{e_t} \mathbf{A}_t^{-H}(1/z^*) \tag{17}$$

where $\mathbf{A}_t(z)$ is a 2×2 matrix with polynomials in each element

$$\mathbf{A}_t(z) = [I - A_t^{(1)} z^{-1} - A_t^{(2)} z^{-2} - A_t^{(3)} z^{-3} - ...] \tag{18}$$

and z^* denotes a complex conjugate of z.

Substituting z with $e^{-i2\pi jf/f_s}$ equation (17) turns into power spectral function

$$\mathbf{P}_t(f) = \frac{1}{f_s} \mathbf{A}_t^{-1}(f) C_{e_t} \mathbf{A}_t^{-H}(f) \tag{19}$$

where f_s is the sampling frequency and $\mathbf{P}_t(f)$ is a 2×2 matrix. The power spectral density (PSD) for RR and RSP can be calculated as absolute values of diagonal elements of $\mathbf{P}_t(f)$

$$P_{RR}(f) = |(\mathbf{P}_t(1,1)(f))| \tag{20}$$

$$P_{RSP}(f) = |(\mathbf{P}_t(2,2)(f))| \tag{21}$$

The off-diagonal elements of $\mathbf{P}_t(f)$ can be used to calculate also phase and coherence spectra, but they are not used in this study.

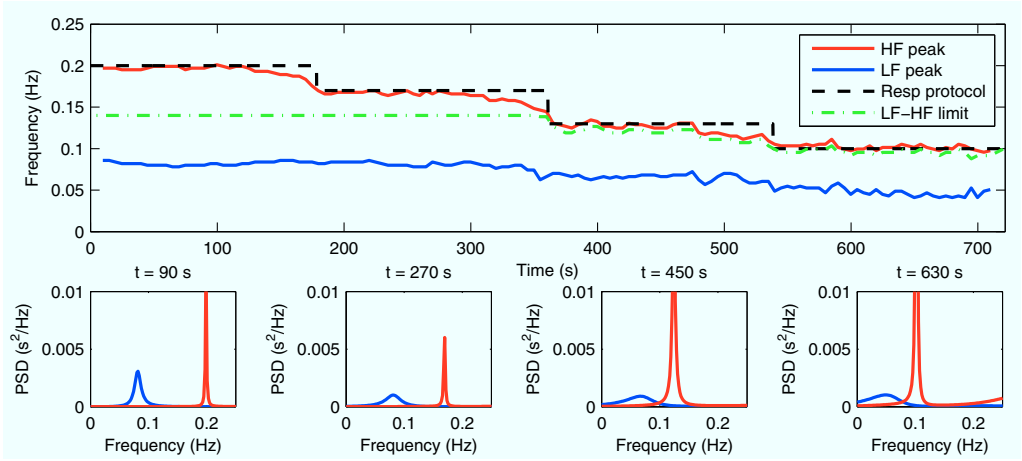

Fig. 1. Upper axes: Respiration protocol and peak frequencies of LF and HF components of RR and LF-HF limit for a single subject. Lower axes: Estimated LF (blue) and HF (red) PSD components from four different time steps.

E. MAR model root factorization

The roots of z-transform (17) can be examined more closely by calculating the inverse matrices (timestep indicator t is left out for clarity)[13].

$$\mathbf{P}(z) = \frac{1}{|\mathbf{A}(z)||\mathbf{A}(1/z^*)|} \begin{bmatrix} \mathbf{A}(2,2)(z) & -\mathbf{A}(1,2)(z) \\ -\mathbf{A}(2,1)(z) & \mathbf{A}(1,1)(z) \end{bmatrix} \cdot C_e \begin{bmatrix} \mathbf{A}(2,2)(1/z^*) & -\mathbf{A}(1,2)(1/z^*) \\ -\mathbf{A}(2,1)(1/z^*) & \mathbf{A}(1,1)(1/z^*) \end{bmatrix}^H \quad (22)$$

where $|\mathbf{A}(z)|$ is determinant of $\mathbf{A}(z)$. This means that there is the same root polynomial $|\mathbf{A}(z)||\mathbf{A}(1/z^*)|$ in denominator for each auto and cross spectra i.e. the poles of each spectra are the same and only the zeros changes according to the matrix multiplication. It should be noted, that MAR model spectrum has zeros even though it does not have moving average (MA) part. Single variable AR model spectrum has only poles and not zeros.

For example the PSD for RR can be calculated from polynomial equation

$$\mathbf{P}_{RR}(z) = [\mathbf{A}(2,2)(z)C_e(1,1)\mathbf{A}(2,2)(1/z^*) - \mathbf{A}(1,2)(z)C_e(2,2)\mathbf{A}(1,2)(1/z^*)]/(|\mathbf{A}(z)||\mathbf{A}(1/z^*)|) \quad (23)$$

By solving the roots of polynomials in numerator and denominator, this can be presented as

$$\mathbf{P}_{RR}(z) = \rho_e \frac{\prod_{i=1}^{I}(z-\beta_i)(1/z-\beta_i^*)}{\prod_{k=1}^{K}(z-\alpha_k)(1/z-\alpha_k^*)} \quad (24)$$

where α_k are the poles, β_i are the zeros and ρ_e is a corresponding element of C_e. Because ρ_e is different for parts that are from auto-coefficients ($\mathbf{A}(2,2)$) and cross-coefficients ($\mathbf{A}(1,2)$), calculation was done separately and the pole spectra were summed together afterwards.

Spectrum estimates for each individual pole were calculated as

$$\mathbf{P}_k(z) = c_k \rho_e \frac{\prod_{i=1}^{I}(z-\beta_i)(1/z-\beta_i^*)}{(z-\alpha_k)(1/z-\alpha_k^*)} \quad (25)$$

where c_k is a coefficient that scales the power to be same as in full PSD in the frequency of the pole

$$c_k = \left. \frac{1}{\prod_{l\neq k}(z_k-\alpha_l)(1/z_k-\alpha_l^*)} \right|_{z_k=e^{-i2\pi f_k/f_s}} \quad (26)$$

where f_k is the frequency of pole α_k.

To prevent any unwanted power generated by the zeros to frequencies far from the pole the individual pole spectra were multiplied with 1 Hz wide Hanning window that was placed on the frequency of the pole.

F. LF and HF components

The respiration frequency for each time step was determined as the frequency of maximum power of the RSP PSD (21). The limit frequency of LF and HF poles was set to be 0.01 Hz lower than respiration frequency. If the RSP frequency was higher than 0.15 Hz the limit was set to 0.14 Hz. The spectra from poles above the limit were summed to be the HF component and the spectra below the limit were summed to be LF component.

The components were estimated for every 5 second for breathing frequencies $0.2-0.1$ Hz to see how the algorithm works when HF frequency gets closer to LF frequency and the components start to overlap.

III. RESULTS

The breathing protocol, estimated peak frequencies for LF and HF components and the LF-HF limit frequency are presented in Fig. 1. There are also samples of estimated component powers for each breathing frequency. The components are clearly separated even when the peaks are close to each other (LF: 0.07 Hz and HF: 0.10 Hz).

In Fig. 2 the protocol and peak frequencies for LF and HF components are presented for all three subjects. There are also the corresponding LF and HF component powers presented in natural logarithmic scale. The HF power increases while the HF frequency decreases. At the same time the LF power stays almost at the same level.

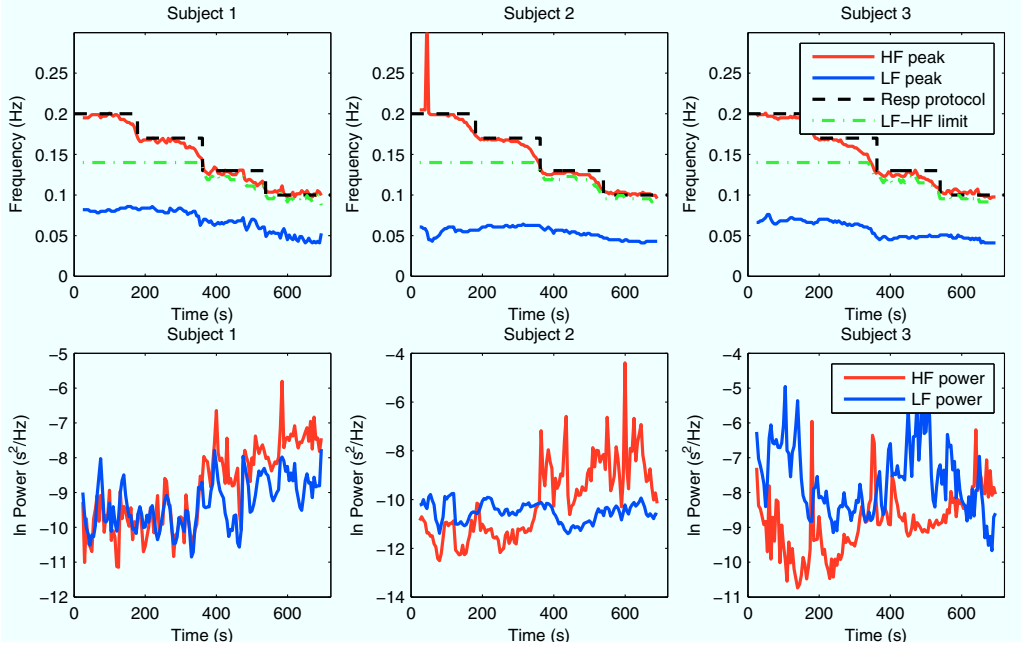

Fig. 2. Upper axes: LF (blue) and HF (red) peak frequencies of RR and LF-HF limit during respiration protocol for 3 subjects. Lower axes: Power values in natural logarithmic scale for LF (blue) and HF (red) components from the corresponding measurement on the upper figures. The rapid change in HF peak frequency at the start of the protocol with subject 2 is probably caused by the adaptation of the algorithm and low HF power.

IV. DISCUSSION

The presented method enables dynamic estimation of the LF and HF component of RR time series with MAR model. From the figures can be seen that the HF frequency tracks the breathing frequency fairly well on every subject while the LF frequency stays approximately at the same level.

The increase of HRV when respiration frequency decreases (in Fig. 2) has been previously reported [14], [15]. However, the results of this study indicate that it is result of increase in HF component power rather than in LF component power. Traditionally calculated LF power would distort when the HF power overlaps with selected LF frequency band.

Due to the spectral decomposition, reliable component powers are obtained even when LF and HF components overlap. Also the individual pole spectra can be divided into those resulted from MAR auto-coefficients (from RR) and those resulted from MAR cross-coefficients (from RSP). This can give more information on how greatly the respiration affects on the HRV.

REFERENCES

[1] Task Force of the European Society of Cardiology and the North American Society of Pacing and Electrophysiology, "Heart rate variability standards of measurement, physiological interpretation, and clinical use," *Circulation*, vol. 93, pp. 1043–1065, 1996.

[2] G. Berntson, "Heart rate variability: Origins, methods and interpretive caveats," *Psychophysiology*, vol. 34, pp. 623–648, 1997.

[3] G. Baselli, S. Cerutti, S. Civardi, D. Liberati, F. Lombardi, A. Malliani, and M. Pagani, "Spectral and cross-spectral analysis of heart rate and arterial blood pressure variability signals," *Computers and Biomedical Research*, vol. 19, no. 6, pp. 520–534, 1986.

[4] G. Baselli, A. Porta, G. Ferrari, S. Cerutti, O. Rimoldi, M. Pagani, and A. Malliani, "Multivariate arma spectral decomposition in the assessment of cardiovascular variabilities," in *Computers in Cardiology 1993, Proceedings.* IEEE, 1993, pp. 731–734.

[5] R. Barbieri, R. Waldmann, V. Di Virgilio, J. Triedman, A. Bianchi, S. Cerutti, and J. Saul, "Continuous quantification of baroreflex and respiratory control of heart rate by use of bivariate autoregressive techniques," *Annals of Noninvasive Electrocardiology*, vol. 1, no. 3, pp. 264–277, 1996.

[6] G. Baselli, A. Porta, O. Rimoldi, M. Pagani, and S. Cerutti, "Spectral decomposition in multichannel recordings based on multivariate parametric identification," *Biomedical Engineering, IEEE Transactions on*, vol. 44, no. 11, pp. 1092–1101, 1997.

[7] V. D. Virgilio, R. Barbieri, L. Mainardi, S. Strano, and S. Cerutti, "A multivariate time-variant AR method for the analysis of heart rate and arterial blood pressure," *Medical Engineering & Physics*, vol. 19, no. 2, pp. 109–124, 1997.

[8] M. Arnold, W. H. R. Miltner, and H. Witte, "Adaptive ar modeling of nonstationary time series by means of kalman filtering," *IEEE Transactions on biomedical engineering*, vol. 45, no. 5, pp. 553–562, 1998.

[9] M. Tarvainen, S. Georgiadis, J. Lipponen, M. Hakkarainen, and P. Karjalainen, "Time-varying spectrum estimation of heart rate variability signals with kalman smoother algorithm," in *Engineering in Medicine and Biology Society, 2009. EMBC 2009. Annual International Conference of the IEEE.* IEEE, 2009, pp. 1–4.

[10] J. Niskanen, M. Tarvainen, P. Ranta-aho, and P. Karjalainen, "Software for advanced hrv analysis," *Computer methods and programs in biomedicine*, vol. 76, no. 1, pp. 73–81, 2004.

[11] M. P. Tarvainen, P. O. Ranta-aho, and P. A. Karjalainen, "An advanced detrending method with application to HRV analysis," *IEEE Transactions on Biomedical Engineering*, vol. 49, no. 2, pp. 172–175, 2002.

[12] M. Tarvainen, S. Georgiadis, P. Ranta-aho, and P. Karjalainen, "Time-varying analysis of heart rate variability signals with a kalman smoother algorithm," *Physiological measurement*, vol. 27, no. 3, p. 225, 2006.

[13] S. L. Marple, *Digital Spectral Analysis*. Prentice-Hall, 1987.

[14] H. Song and P. Lehrer, "The effects of specific respiratory rates on heart rate and heart rate variability," *Applied psychophysiology and biofeedback*, vol. 28, no. 1, pp. 13–23, 2003.

[15] B. Aysin and E. Aysin, "Effect of respiration in heart rate variability (hrv) analysis," in *Engineering in Medicine and Biology Society, 2006. EMBS'06. 28th Annual International Conference of the IEEE.* IEEE, 2006, pp. 1776–1779.